J Physiol Sci (2016) 66:53–65
DOI 10.1007/s12576-015-0393-4

ORIGINAL PAPER

Effects of ezrin knockdown on the structure of gastric glandular epithelia

Saori Yoshida[1] · Hiroto Yamamoto[1,2] · Takahito Tetsui[1] · Yuka Kobayakawa[1] · Ryo Hatano[1] · Ken-ichi Mukaisho[2] · Takanori Hattori[2] · Hiroyuki Sugihara[2] · Shinji Asano[1]

Received: 4 May 2015 / Accepted: 18 August 2015 / Published online: 2 September 2015

Abstract Ezrin, an adaptor protein that cross-links plasma membrane-associated proteins with the actin cytoskeleton, is concentrated on apical surfaces of epithelial cells, especially in microvilli of the small intestine and stomach. In the stomach, ezrin is predominantly expressed on the apical canalicular membrane of parietal cells. Transgenic ezrin knockdown mice in which the expression level of ezrin was reduced to <7 % compared with the wild-type suffered from achlorhydria because of impairment of membrane fusion between tubulovesicles and apical membranes. We observed, for the first time, hypergastrinemia and foveolar hyperplasia in the gastric fundic region of the knockdown mice. Dilation of fundic glands was observed, the percentage of parietal and chief cells was reduced, and that of mucous-secreting cells was increased. The parietal cells of knockdown mice contained dilated tubulovesicles and abnormal mitochondria, and subsets of these cells contained abnormal vacuoles and multilamellar structures. Therefore, lack of ezrin not only causes achlorhydria and hypergastrinemia but also changes the structure of gastric glands, with severe perturbation of the secretory membranes of parietal cells.

Keywords Ezrin · Parietal cells · Epithelium · Secretory membrane

Introduction

The ERM (ezrin, radixin, and moesin) family of proteins are adaptor proteins that cross-link between plasma membrane-associated proteins (for example adhesion proteins and transport proteins) and the actin cytoskeleton. These proteins bind to membrane proteins directly or indirectly via scaffold proteins at the specific binding domain (termed the FERM domain) located at the N-terminal part, and to F-actin at the major actin-binding site located at the C-terminal part [1–3]. They are important in the formation of microvilli, filopodia, uropods, and ruffling membranes, where actin filaments are associated with plasma membranes [4]. The cross-linking activity of ERM proteins is regulated by their own intra or intermolecular interaction. In the dormant form of ERM proteins, interaction between their N and C-terminal domains results in masking of their binding sites to actin filaments and membrane-associated proteins [5, 6]. Phosphorylation of their C-terminal threonine residue (Thr^{567} in ezrin, Thr^{564} in radixin, and Thr^{558} in moesin) by Rho kinase or protein kinase C, and phosphatidyl inositol 4,5-bisphosphate binding to their N-terminal FERM domain open up the dormant conformation into the active open conformation. In this process, the ERM proteins are recruited from the cytoplasm (as a soluble and inactive form) to the membrane (as an insoluble and active form).

One of the ERM family proteins, ezrin, is highly concentrated on the apical surfaces of many epithelial cell types, especially in the small and large intestine, stomach, kidneys, and lungs [7]. In the stomach, ezrin, located

Electronic supplementary material The online version of this article (doi:10.1007/s12576-015-0393-4) contains supplementary material, which is available to authorized users.

✉ Shinji Asano
ashinji@ph.ritsumei.ac.jp

[1] Department of Molecular Physiology, College of Pharmaceutical Sciences, Ritsumeikan University, 1-1-1 Noji-Higashi, Kusatsu, Shiga 525-8577, Japan

[2] Department of Pathology, Shiga University of Medical Sciences, Seta Tsukinowa-cho, Otsu, Shiga 520-2192, Japan

especially in parietal cells, is predominantly expressed on the apical canalicular membranes [8]. It is involved in remodeling of the apical surface membrane and in gastric acid secretion [9]. Protein kinase A-mediated phosphorylation of ezrin at the N-terminal Ser^{66} opens up the dormant conformation into the active open conformation, and is essential for gastric acid secretion stimulated by histamine [10].

The function of ezrin in vivo was originally studied by use of knockout (*Vil2*$^{-/-}$) mice. In neonatal *Vil2*$^{-/-}$ mice, microvilli formation in the small intestine was observed whereas organization of the terminal web region of the small intestine was impaired [11]. However, the *Vil2*$^{-/-}$ mice did not survive past weaning. Recently, Casaletto et al. [12] studied mice with conditional knockout of the *Vil2* gene and observed that ezrin is necessary for intestinal development and homeostasis, especially in villus morphogenesis and maintenance. Tamura et al. [13] prepared ezrin knockdown (*Vil2*$^{kd/kd}$) mice in which the level of expression of ezrin was reduced to <7 % compared with wild-type mice. Severe growth retardation and high mortality up to their weaning period was observed for the *Vil2*$^{kd/kd}$ mice. Grown-up *Vil2*$^{kd/kd}$ mice suffered from achlorhydria because of impairment of secretagogue-stimulated membrane fusion of gastric tubulovesicles with the apical plasma membrane [13]. However, the effects of knockdown of ezrin expression on the structure of gastric epithelia have not yet been studied. Here, we studied the structure of the gastric epithelia of *Vil2*$^{kd/kd}$ mice, and found, for the first time, foveolar hyperplasia, dilation of fundic glands, a decrease in the percentages of chief and parietal cells, and an increase in the percentage of neck cells. We also found severe perturbations in the secretory membranes of the parietal cell in the *Vil2*$^{kd/kd}$ mice, including dilated tubulovesicles, vacuolation, and abnormal multilamellar structure.

Materials and methods

Generation of *Vil2*$^{kd/kd}$ mice

Vil2$^{kd/kd}$ mice were kind gifts from Professor Tsukita of the Graduate School of Frontier Biosciences, Osaka University. Up to the weaning period, mortality of the mice was high, as reported elsewhere [13]. However, technical improvement of our handling and feeding methods successfully reduced mortality at 50 days after birth from 93 to 80 %, which enabled us to study the phenotypes of adult mutant mice [14]. Genotyping of mice was performed by PCR of mouse genomic DNA, by using a combination of primers specific for the wild-type allele and for the targeted allele. The forward and reverse primers for the wild-type allele were 5′-GTGTGGCACTCTGCCTTCAAG-3′ and 5′-CATGGTGCCACACAGGACTC-3′, respectively. The reverse primer for the targeted allele was 5′-AGCGGATCTCAAACTCTCCTC-3′. In this study, 8-week-old female mice were used. The mRNA expression levels of ezrin in the gastric corpus and pyloric antrum segments of *Vil2*$^{kd/kd}$ mice were 2.1 and 4.4 %, respectively, compared with those of wild-type mice (supplementary Fig. 1).

Antibodies

Monoclonal anti-ezrin (3C12), anti-Ki67 (ab16667) antibodies, and a rabbit polyclonal anti-gastric intrinsic factor (GIF) (ab91322) were purchased from Abcam (Cambridge, UK). Monoclonal anti-gastric proton pump α-subunit (1H9) and β-subunit (2B6) antibodies were purchased from Medical and Biological Laboratories (Nagoya, Japan). A rabbit polyclonal anti-pepsin C (H-56) antibody was purchased from Santa Cruz Biotechnology (Santa Cruz, CA, USA). A monoclonal anti-OxPhos Complex IV subunit I (1D6E1A8) antibody was purchased from Invitrogen (Camarillo, CA, USA).

Measurement of serum gastrin levels

Mice were starved for 16 h before blood sampling. Blood was collected from the mouse hearts, coagulated, and centrifuged at 2000×*g* for 20 min to obtain serum. Serum gastrin levels were determined by radioimmunoassay.

Histochemical studies with antibodies and lectin

Mouse stomachs were excised along the greater curvature and dissected into three segments; fundus, corpus, and pyloric antrum. For immunohistochemistry, mouse tissue samples were fixed in a paraformaldehyde-based fixing solution, overnight at 4 °C, embedded in paraffin, and cut into sections 4-μm-thick. Deparaffined and rehydrated slices were subjected to antigen retrieval by boiling for 45 min in Immunosaver (Nisshin EM, Tokyo, Japan), then treatment with 3 % H_2O_2 in methanol for 20 min at room temperature. Slides were washed in phosphate-buffered saline (PBS), and then sections were incubated overnight at 4 °C with primary antibodies. Slides were washed in PBS, then incubated for 30 min at room temperature with a horseradish peroxidase-conjugated goat anti-mouse or anti-rabbit IgG (Nichirei Bioscience, Tokyo, Japan). After washing with PBS, antibody binding was detected by use of 3,3′-diaminobenzidine solution (Nichirei Bioscience, Tokyo, Japan). The tissue sections were counterstained with hematoxylin. To reveal mucin, tissue sections were stained with periodic acid–Schiff (PAS) or Concanavalin A (Con A).

For lectin staining, slides were incubated for 30 min at room temperature with a biotin-conjugated *Griffonia*

simplicifolia lectin (GS-II; EY Laboratories, San Mateo, USA) instead of primary antibodies. They were washed in PBS then incubated for 30 min at room temperature with horseradish peroxidase-conjugated streptoavidin (Nichirei Bioscience). After washing with PBS, slides were incubated with 3,3′-diaminobenzidine solution (Nichirei Bioscience, Tokyo, Japan).

Immunofluorescence microscopy

Mouse tissue samples were prepared, fixed, embedded, sliced, and deparaffined as reported in the section on histochemical studies. Deparaffined and rehydrated slices were subjected to antigen retrieval by boiling for 45 min in Immunosaver (Nisshin EM) then treatment with 10 % goat serum for 30 min at room temperature. Slides were washed in PBS, then sections were incubated with primary antibodies overnight at 4 °C. Slides were washed with PBS containing 0.03 % Tween 20 (PBS-T) then incubated with Alexa Fluor 488-labeled goat anti-mouse IgG (H+L), Alexa Fluor 594-labeled goat anti-rabbit IgG (H+L), and 1 μg/ml DAPI at room temperature for 1 h. After washing with PBS-T, the sections were mounted with fluorescent mounting medium (Vectashield, Vector Laboratories, CA, USA) and examined by use of a confocal laser scanning microscope (FV-1000D IX-81; Olympus, Tokyo, Japan).

RNA preparation and quantitative RT-PCR

Total RNA samples from mouse tissues were prepared by use of an Isogen (Nippon Gene, Tokyo, Japan), in accordance with the manufacturer's instructions. Total RNA samples were reverse-transcribed, by use of an oligo $d(T)_6$ primer, to prepare cDNA samples with an Omniscript RT kit (Qiagen). The cDNA samples were used as templates for quantitative RT-PCR.

Quantitative RT-PCR for mouse gastric proton pump α and β subunits (*ATP4a* and *ATP4b*), gastric intrinsic factor (GIF), pepsinogen I, anion exchanger AE2, SP/TFF2, MUC6, COX-2, TNF-α, IL-1β, and glyceroaldehyde-phosphate dehydrogenase (GAPDH) was performed by use of the SYBR Premix Ex Taq (Takara Bio); the gene-specific primers used are listed in Table 1. The expression level of each mRNA was normalized to the expression level of GAPDH. Identities of amplified PCR products were confirmed by use of agarose or polyacrylamide gel electrophoresis.

Table 1 PCR primers for quantitative RT-PCR

Gastric proton pump α-subunit (*ATP4a*)
Forward primer, 5′-AGATGTCCTCATCCGCAAGACAC-3′
Reverse primer, 5′-CAGCCAATGCAGACCTGGAA-3′
Gastric proton pump β-subunit (*ATP4b*)
Forward primer, 5′-TGGCACCTTCAGTCTCCACTATTTC-3′
Reverse primer, 5′-ATCTTGCACACGATGCTGACTTG-3′
Anion exchanger 2 (AE2)
Forward primer, 5′-CACCACCCAGATGTCACCTATGTC-3′
Reverse primer, 5′-CCAGGCAGAGCAACTGCAAG-3′
Gastric intrinsic factor (GIF)
Forward primer, 5′-CATCCTGATTGCCATGAACCTG-3′
Reverse primer, 5′-GCCATAACGGTGAGGGCAAG-3′
Pepsinogen C
Forward primer, 5′-ACCCAGGAGCTTTACTGGCAGA-3′
Reverse primer, 5′-CAGGTACTGGGCAGGCATGA-3′
Mucin 6 (MUC6)
Forward primer, 5′-TTCCTGAGCCGCAGCACTT-3′
Reverse primer, 5′-CAGAAACCCTGGCAACGAGTTAG-3′
TFF2
Forward primer, 5′-TTGATCTTGGATGCTGCTTTGAC-3′
Reverse primer, 5′-GCGAGCTGACACTTCCATGAC-3′
COX2
Forward primer, 5′-TGGTTACAAAAGCTGGGAAGC-3′
Reverse primer, 5′-ATGGGAGTTGGGCAGTCATC-3′
TNF-α
Forward primer, 5′-GACTAGCCAGGAGGGAGAACAGA-3′
Reverse primer, 5′-CCTGGTTGGCTGCTTGCTT-3′
IL-1β
Forward primer, 5′-TCCAGGATGAGGACATGAGCAC-3′
Reverse primer, 5′-GAACGTCACACACCAGCAGGTTA-3′
Glyceraldehyde-phosphate dehydrogenase (GAPDH)
Forward primer, 5′-TGTGTCCGTCGTGGATCTGA-3′
Reverse primer, 5′-TTGCTGTTGAAGTCGCAGGAG-3′

Electron microscopy

Samples were fixed with 2 % paraformaldehyde and 2 % glutaraldehyde in 0.1 M phosphate buffer, pH 7.4 (PB) at 4 °C overnight. After the samples had been washed three times with 0.1 M PB, they were post-fixed with 2 % osmium tetraoxide in 0.1 M PB at 4 °C for 2 h. The post-fixed samples were successively dehydrated in 50, 70, 90, and 100 % ethanol, infiltrated twice with propylene oxide (PO), and placed in a 70:30 mixture of PO and resin (Quetol-812; Nisshin EM) for 1 h. PO was volatilized overnight. The samples were transferred to a fresh 100 % resin, and polymerized at 60 °C for 2 days. The polymerized resins were ultra-thin sectioned at 70 nm, and the sections were mounted on copper grids. They were stained with 2 % uranyl acetate at room temperature for 15 min, and then washed with distilled water followed by secondary staining with lead stain solution (Sigma–Aldrich, Tokyo, Japan) at room temperature for 3 min. The grids were observed by transmission electron microscopy (JEM-1400Plus; Jeol, Tokyo, Japan).

Results

Expression of ezrin in the gastric mucosa

In wild-type gastric mucosa, ezrin was expressed in the corpus and pyloric antrum segments (Fig. 1a). In the gastric corpus, ezrin was mainly expressed in parietal cells which can be stained with an anti-proton pump α-subunit antibody (Fig. 1b, c). Ezrin also seems to be expressed in the surface mucous cells which line the surface and the gastric pits, although its expression level was much lower than that in parietal cells. In the pyloric antrum segments, ezrin was also expressed in the pyloric gland where the gastric proton pump α-subunit was apparently absent (Fig. 1a). In this work, we studied the structure of the gastric epithelia of *Vil2*$^{kd/kd}$ mice.

Phenotypes of *Vil2*$^{kd/kd}$ mice

As reported elsewhere, growth of *Vil2*$^{kd/kd}$ mice was severely retarded; the body weight of 8-week-old *Vil2*$^{kd/kd}$ mice was 20 % less than that of their wild-type litter mates (14.4 ± 0.5 g for *Vil2*$^{kd/kd}$ mice, and 17.8 ± 0.5 g for wild-type mice). Grown-up *Vil2*$^{kd/kd}$ mice suffered from achlorhydria because of impairment of secretagogue-stimulated membrane fusion of gastric intracellular tubulovesicles with the apical plasma membrane [13]. The mice also had abnormalities of phosphate and calcium handling, because of reduced membrane expression of Na^+/P_i co-transporters (Npt2a) in the renal proximal tubules and TRPV6 channel in the duodenum [14]. Very recently we reported that the mice developed severe intrahepatic cholestasis because of impairment of cell surface expression of cystic fibrosis transmembrane regulator (CFTR), anion exchanger (AE2), and aquaporin (AQP1) in cholangiocytes [15].

Serum gastrin of *Vil2*$^{kd/kd}$ mice

The peptide hormone gastrin is important in the regulation of acid secretion, and in the proliferation and differentiation of gastric mucosa [16]. Ezrin has been identified as a major target of gastrin in immature gastric parietal cells [17]. Plasma concentrations of gastrin were elevated (hypergastrinemia) in several mouse models of achlorhydria [18–21]. In this study we measured serum gastrin concentrations to compare levels in *Vil2*$^{kd/kd}$ and wild-type mice. Serum gastrin concentrations of *Vil2*$^{kd/kd}$ mice were 2.8-times higher than those of wild-type mice (wild-type, 98 ± 48 pg/ml ($N = 4$); *Vil2*$^{kd/kd}$, 277 ± 103 pg/ml ($N = 5$)). Therefore, *Vil2*$^{kd/kd}$ mice had both hypergastrinemia and achlorhydria, as was found for mice with targeted disruption of the gastric proton pump [19, 20], NHE2 [18] and KCNE2 [21].

Fig. 1 Expression of ezrin and gastric proton pump α-subunit in the gastric corpus and pyloric antrum segments. **a** Sections of gastric corpus and pyloric antrum segments of wild-type mice were stained with the anti-ezrin and anti-gastric proton pump α-subunit antibodies, respectively. The patterns were shown by staining with DAB. *Scale bar* 100 μm. **b**, **c** Immunofluoresence observation of the gastric corpus of wild-type and *Vil2*$^{kd/kd}$ mice with the anti-ezrin (*red*), anti-gastric proton pump α-subunit antibodies (*green*) and DAPI (*blue*), respectively at low (**b**) and high (**c**) magnification. Immunofluoresence of the bottom part of the gastric corpus is shown in (**c**). *Scale bars* 100 μm (**b**, **c**)

Enlarged gastric epithelial region and dilation of gastric glands in *Vil2*$^{kd/kd}$ mice

Vil2$^{kd/kd}$ mice had markedly enlarged stomachs although their total body weight was 20 % less than that of their litter mates. Stomach weight of *Vil2*$^{kd/kd}$ mice was approximately 60 % larger than that of wild-type mice: 0.26 ± 0.01 g ($N = 4$) and 0.16 ± 0.03 g ($N = 4$), respectively. Therefore, the stomach weight relative to total body weight for *Vil2*$^{kd/kd}$ mice was twice as large as that for wild-type mice, as reported for gene targeting of *Atp4a* (gastric proton pump α subunit) and *Kcne2* [21, 22]. Figures 2a, b show hematoxylin and eosin staining patterns of the gastric corpus of wild-type and *Vil2*$^{kd/kd}$ mice. The thickness of the gastric epithelial region of *Vil2*$^{kd/kd}$ mice (471 ± 14 μm; $N = 4$ animals) was larger than that of their wild-type litter mates (320 ± 4 μm; $N = 3$ animals) at the age of 8 weeks. This was mainly because of a marked increase in number of surface mucous cells, as a result of foveolar hyperplasia. In fact, many more surface cells were stained with PAS in the *Vil2*$^{kd/kd}$ mice (Fig. 2c, d). The fundic gland was dilated, and the number of cells in the gland was increased. Foveolar hyperplasia in the *Vil2*$^{kd/kd}$ stomach was accompanied by a significant increase in the number of cells stained with an antibody against a proliferative nuclear marker, Ki67, especially in the isthmus region (progenitor zone) [23]. Ki-67-positive cells were also sporadically found in the base of the gland of *Vil2*$^{kd/kd}$ mice. (Fig 3).

Reduced percentage of parietal, chief cells and increased percentage of neck cells in *Vil2*$^{kd/kd}$ mice

The fundic gland is composed of several types of cell: parietal cells, chief (zymogenic) cells, and mucous secreting (neck) cells. The proportions of these types of cell in the gastric gland were compared for wild-type and *Vil2*$^{kd/kd}$ mice (Table 2). Parietal cells were stained with an

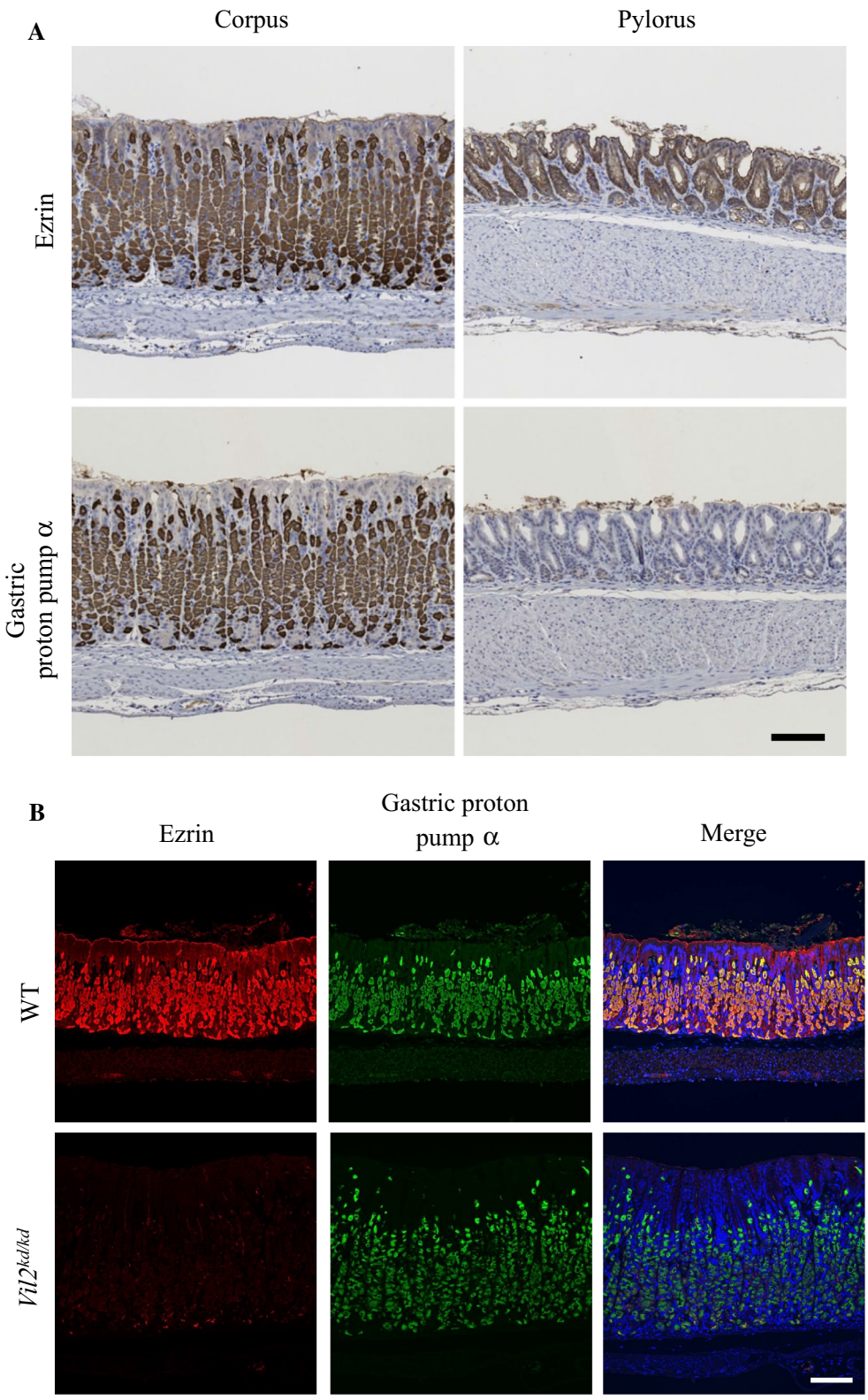

antibody against proton pump α subunit (HK-α) (Fig. 4a, b). Chief cells were stained with an antibody against pepsin C (Fig. 4c, d). Mucous neck cells were stained with lectin GSII (Fig. 4e, f) [24, 25]. These cells can be also stained with Con A (supplementary Fig. S2). The percentage of parietal cells per gastric fundic gland was significantly

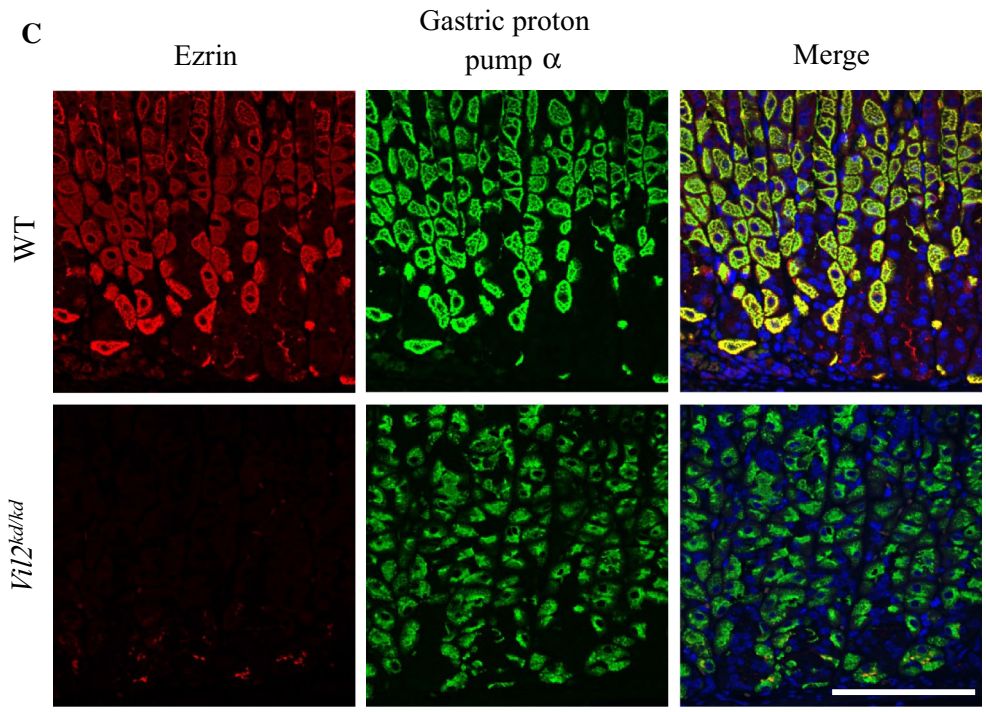

Fig. 1 continued

reduced in *Vil2*$^{kd/kd}$ mice compared with wild-type mice (Table 2). Percentage of chief cells per fundic gland was also significantly reduced in *Vil2*$^{kd/kd}$ mice compared with wild-type mice. In contrast, the number of mucous neck cells was significantly increased in *Vil2*$^{kd/kd}$ mice compared with wild-type mice. It should be noted that the parietal cells of *Vil2*$^{kd/kd}$ mice had irregular (small and condensed) shapes (Fig. 4a, b).

We also measured the mRNA expression levels of marker proteins for parietal and chief cells to compare the levels for *Vil2*$^{kd/kd}$ and wild-type mice. mRNA expression levels of gastric proton pump α and β subunits in the stomach of *Vil2*$^{kd/kd}$ mice decreased to 57 ± 10 and 45 ± 11 %, respectively, compared with those found in their wild-type litter mates (Fig. 5). We also measured the mRNA levels of the anion exchanger AE2, a transporter directly involved in gastric acid secretion in parietal cells, again to compare levels for *Vil2*$^{kd/kd}$ and wild-type mice, because targeted disruption of AE2 in mice also impaired gastric acid secretion [26]. The mRNA expression level of AE2 in the stomach of *Vil2*$^{kd/kd}$ mice also decreased to 48 ± 11 % of the level for their wild-type litter mates (Fig. 5). mRNA expression levels of pepsinogen and GIF in the stomach of *Vil2*$^{kd/kd}$ mice also decreased to 25 ± 3 and 43 ± 7 %, respectively, of the levels in their wild-type litter mates (Fig. 5). These results are in good agreement with decreased percentages of parietal and chief cells in fundic glands.

The loss of functional parietal cells has been reported to lead to changes in cell lineages in the gastric mucosa, including foveolar hyperplasia, mucous cell metaplasia, and spasmolytic polypeptide (SP)-expressing metaplasia (SPEM) [27]. SPEM is indicative of metaplastic glands in the fundus with a phenotype similar to that of antral or pyloric glands [28]. Trefoil factor family peptides 2 (TFF2) and a mucin glycoprotein, MUC6, which are co-localized in the deep antral glands of stomach [29], are regarded as markers of SPEM [27]. However, mRNA expression levels of SP/TFF2 and MUC6 in the gastric fundic region of *Vil2*$^{kd/kd}$ mice were unchanged or slightly lower (89 ± 10 and 93 ± 17 %, respectively) compared with the levels in their wild-type litter mates (Fig. 5). These results suggest that the gastric mucosa of *Vil2*$^{kd/kd}$ mice is not indicative of SPEM.

Inflammation markers were not up-regulated in the Vil2$^{kd/kd}$ stomach

There was, apparently, no infiltration of inflammatory cells in the *Vil2*$^{kd/kd}$ stomach (data not shown). We also examined the expression of a variety of inflammation markers in the *Vil2*$^{kd/kd}$ stomach. mRNA levels of COX-2, TNF-α, and IL-1β in the gastric corpus were measured to compare the results for *Vil2*$^{kd/kd}$ and wild-type mice. Expression levels of COX-2, TNF-α, and IL-1β were significantly lower (35 ± 15, 49 ± 10, and 38 ± 19 %, respectively) than

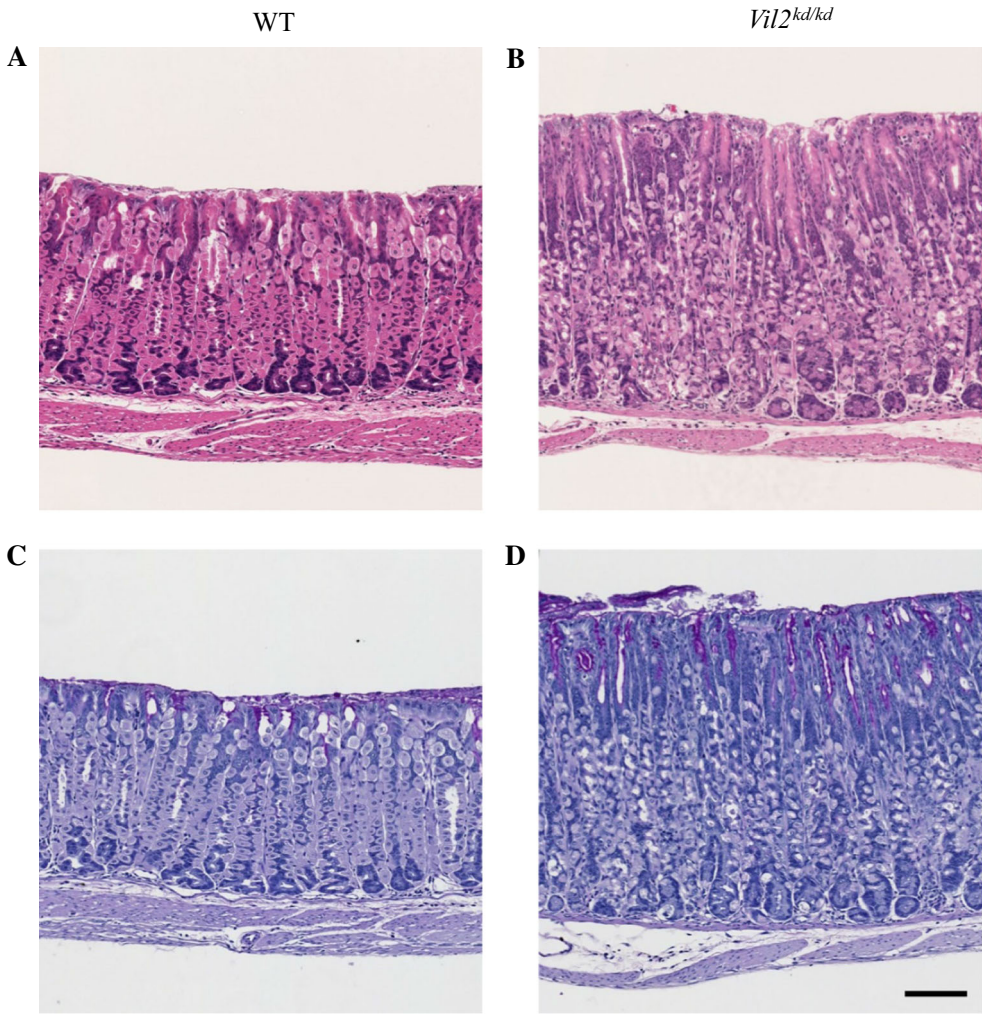

Fig. 2 Foveolar hyperplasia was found in the gastric corpus of *Vil2*$^{kd/kd}$ mice. Sections of the gastric corpus of wild-type (**a**, **c**) and *Vil2*$^{kd/kd}$ mice (**b**, **d**) were stained with H.E. (**a**, **b**) and PAS (**c**, **d**). *Scale bar* 100 μm

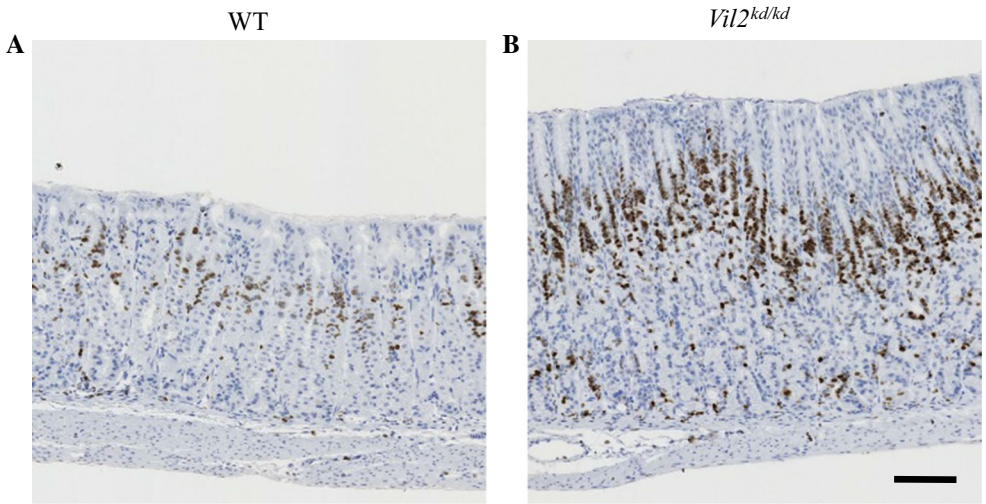

Fig. 3 Expression of Ki-67 in the gastric corpus of wild-type and *Vil2*$^{kd/kd}$ mice. Sections of gastric corpus of wild-type (**a**) and *Vil2*$^{kd/kd}$ (**b**) mice were stained with the anti-Ki-67 antibody. *Scale bar* 100 μm

Table 2 Epithelial cell populations of gastric glands

	Wild-type	*Vil2*$^{kd/kd}$
Parietal cells (%)	40 ± 2	29 ± 1
Chief cells (%)	23 ± 2	14 ± 2
Mucous neck cells (%)	19 ± 2	35 ± 3
Others (%)	18 ± 2	22 ± 2

All values are mean ± SE and are the percentages of the specific cell population of all the cell populations in the glands. $N = 7$ for wild-type, and $N = 8$ for *Vil2*$^{kd/kd}$ mice

those in their wild-type litter mates (Fig. 6). The reason for the down-regulation of these genes cannot yet be explained. These results suggest there is no inflammation in the gastric corpus of *Vil2*$^{kd/kd}$ mice.

Secretory membranes of parietal cells were perturbed in *Vil2*$^{kd/kd}$ mice

Ezrin is phosphorylated by protein kinase A when parietal cells are treated with histamine, and is involved in membrane fusion between gastric tubulovesicles and apical plasma membranes [10]. In this process of membrane fusion, ezrin interacts with an Arf-GTPase-activating protein, ACAP4 [30]. Here we focused on and compared the ultrastructure of parietal cells between wild-type and *Vil2*$^{kd/kd}$ mice. In wild-type parietal cells there were numerous mitochondria and tubulovesicles adjacent to the canaliculi (Fig. 7a, c, e). In contrast, *Vil2*$^{kd/kd}$ parietal cells lacked typical tubulovesicles, and subsets of these cells contained abnormal vacuoles and mitochondria (Fig. 7b, d, f). This result was in good agreements with the finding that labeling with the anti-OxPhos antibody, which binds to active mitochondria in viable cells [31], was down-regulated in *Vil2*$^{kd/kd}$ parietal cells (Fig. 8). These severe perturbations of the secretory membranes of parietal cells have also been observed in mice with knockout of gastric proton pump α subunit, *Atp4a*$^{-/-}$ [20]. It should be noted that abnormal multilamellar structures, which were similar to autophagosomes, were found in the subsets of parietal cells of *Vil2*$^{kd/kd}$ mice (Fig. 7g, h).

Discussion

It has been reported that ezrin is expressed in parietal cells and chief cells of the fundic glands of the mouse stomach [7]. Here we also discovered that ezrin was predominantly expressed in parietal cells stained with anti-gastric proton pump α-subunit antibody (Fig. 1). It was also expressed in the surface mucous cells and at the base of glands, although the expression level was very low. Expression of ezrin at the base of glands was sporadic and partly overlapped expression of pepsin C in chief cells (supplementary Fig. S3). It has been reported that in rabbit gastric glands another ERM protein, moesin, rather than ezrin, was expressed on the apical membrane of chief cells [25]. However, we could not detect such expression of moesin specific for chief cells in mice. It has been reported that ERM proteins share common structural and functional properties, and have functional redundancy [3]. However, moesin was not expressed to compensate the loss of ezrin in the *Vil2*$^{kd/kd}$ parietal cells (supplementary Fig. S4).

As reported elsewhere, *Vil2*$^{kd/kd}$ mice suffered from achlorhydria because of impairment of membrane fusion between intracellular tubulovesicles containing gastric proton pumps and the canalicular membrane at the apical surface of parietal cells [13]. In this work we studied, for the first time, the effect of knockdown of ezrin expression on the structure of gastric epithelia. Several structural changes were observed, not only in parietal cells but also in the whole fundic region of the gastric mucosa of *Vil2*$^{kd/kd}$ mice: foveolar hyperplasia, dilation of glands, a decrease in the percentages of parietal and chief cells, and an increase in the percentage of neck cells. Development of foveolar hyperplasia has been reported in many kinds of knockout mice with achlorhydria [21, 22] and in normal rats treated with the proton pump inhibitor omeprazole [32]. Therefore, the foveolar hyperplasia found in the *Vil2*$^{kd/kd}$ mouse stomach should be a secondary effect of achlorhydria. However, the structural changes were also found in adult *Vil2*$^{kd/kd}$ mice (17 weeks old) drinking diluted acetic acid (pH 3.0) instead of water ad libitum for one week (data not shown). Nomura et al. [33] reported that gastrin was required for induction of foveolar hyperplasia, on the basis that neither foveolar hyperplasia nor proliferative response was observed for gastrin knockout mice. Hypergastrinemia has also been observed for *Vil2*$^{kd/kd}$ mice, and may result in foveolar hyperplasia. The magnitude of the increase in serum gastrin level found in this study was smaller (2.8 fold higher than for wild-type mice) than that found in similar knockout studies (three to sixfold higher than for wild-type mice) [18–21] but comparable with that found for Huntingtin interacting protein-related (Hip1r) knockout mice (2.7 fold higher than for wild-type mice) [34].

Here we also observed a decrease in the percentage of parietal and chief cells and an increase in the percentage of neck cells in *Vil2*$^{kd/kd}$ mice. Similar changes in the structure and development of gastric epithelia have been reported—SP/TFF2 and MUC6 were up-regulated, indicative of SPEM. The SPEM cell lineage was originally differentiated from mucous neck cells at the base region of the fundic glands in the absence of parietal cells. SPEM develops after loss of parietal cells as a result of chronic *Helicobacter* infection and oxyntic atrophy inflammation [35], transgenic expression of the cholera

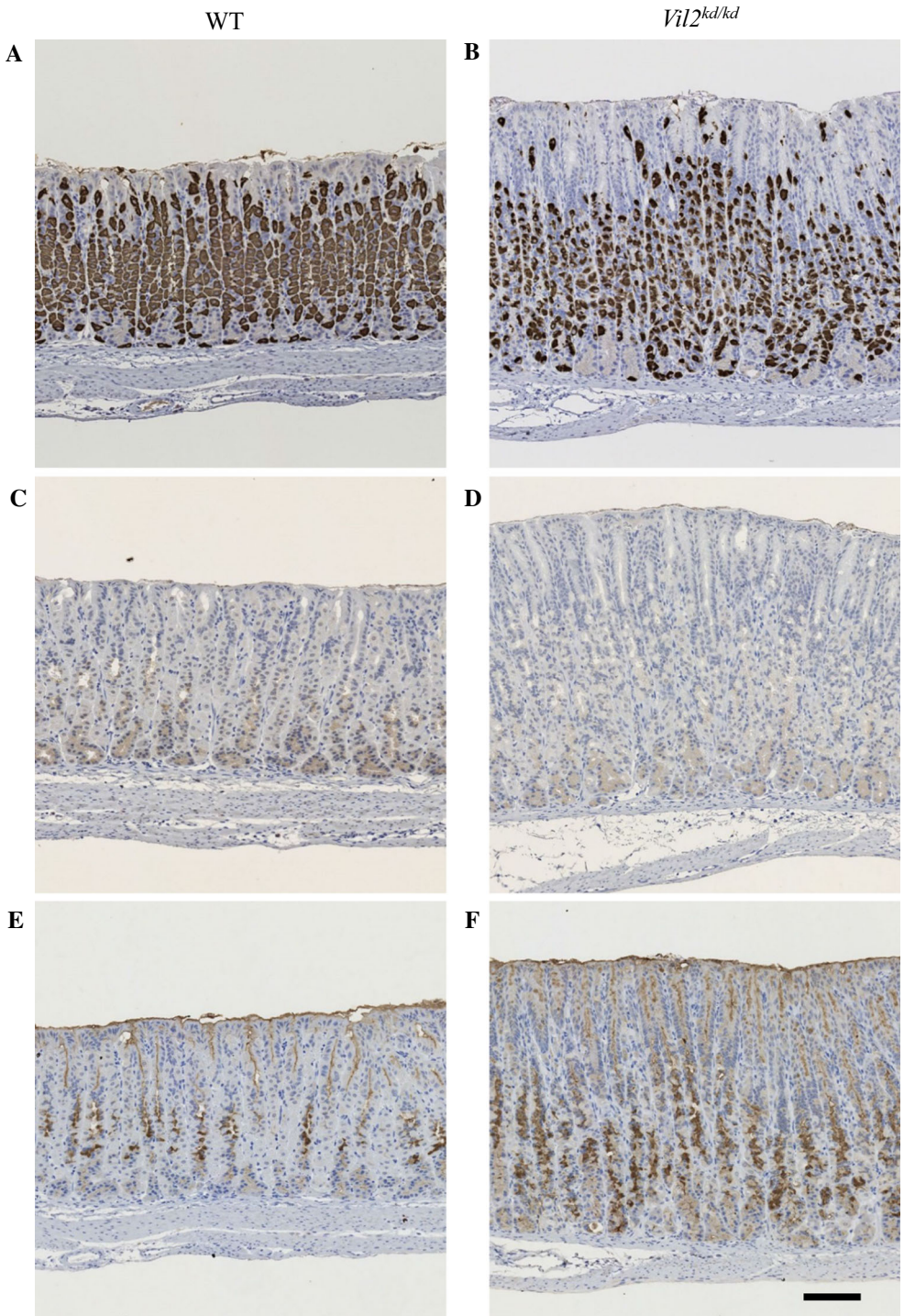

Fig. 4 Expression of gastric proton pump α-subunit, pepsin C, and GSII lectin-positive carbohydrate in the gastric corpus of wild-type and *Vil2*$^{kd/kd}$ mice. Sections of the gastric corpus of wild-type (**a**, **c**, **e**) and *Vil2*$^{kd/kd}$ (**b**, **d**, **f**) mice were stained with the anti-gastric proton pump α-subunit (**a**, **b**) and pepsin C (**c**, **d**) antibodies, respectively. The sections were also stained with GSII (**e**, **f**). *Scale bar* 100 μm. The numbers of proton pump α-subunit, pepsin C, and GSII-positive cells were counted in the gastric gland; their percentages are listed in Table 2

toxin A1 subunit in parietal cells [36], and treatment with DMP-777, which acts as a toxic protonophore for the parietal cell secretory membrane [37]. However, in the fundic region of *Vil2*$^{kd/kd}$ mice, up-regulation of SP/TFF2 and MUC6 was not observed, suggesting that the *Vil2*$^{kd/kd}$ stomach is not indicative of SPEM. This may be because

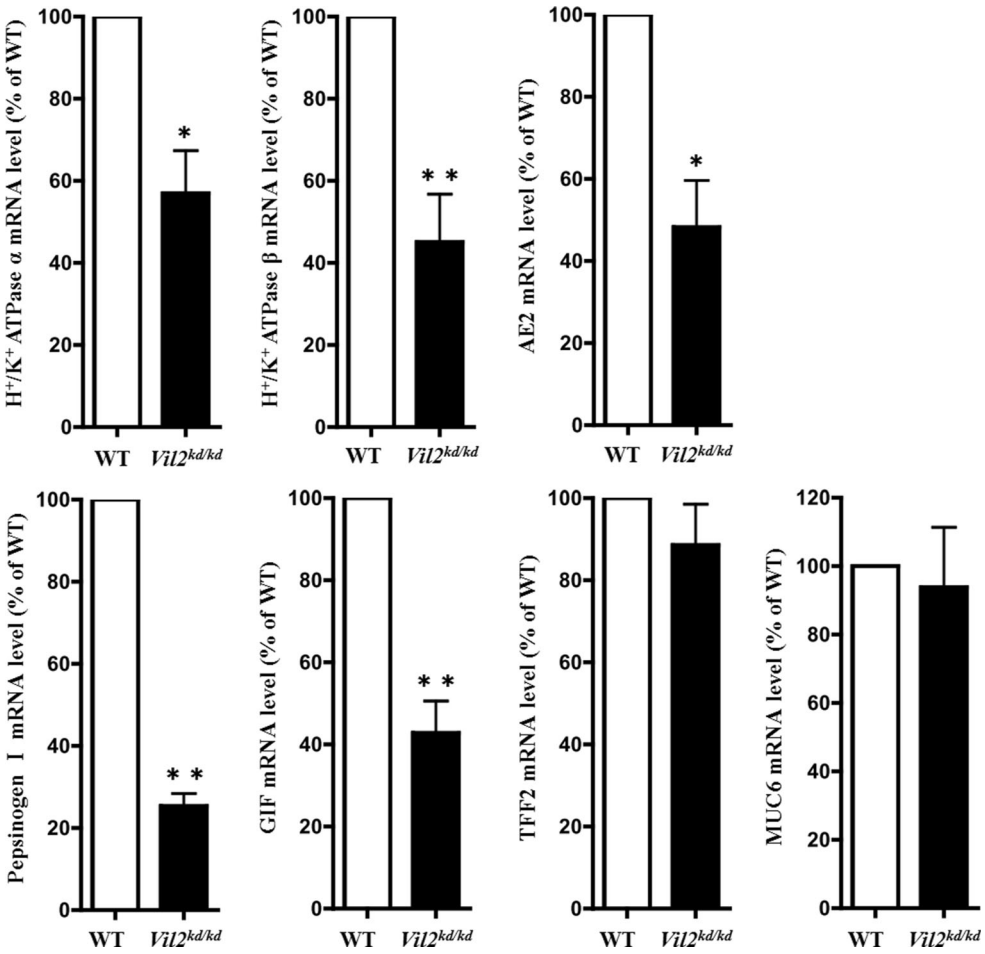

Fig. 5 mRNA expression levels of gastric proton pump α and β subunits, AE2, pepsinogen I, GIF, TFF2, and MUC6 in the gastric corpus were compared between wild-type and *Vil2*$^{kd/kd}$ mice. The mRNA expression levels were normalized to the level of expression of GAPDH, and values are shown as percentages of the expression levels in the wild-type. All values are mean ± SE, $N = 3$, for wild-type and *Vil2*$^{kd/kd}$ mice. $^{*}P < 0.05$ and $^{**}P < 0.01$ versus wild-type

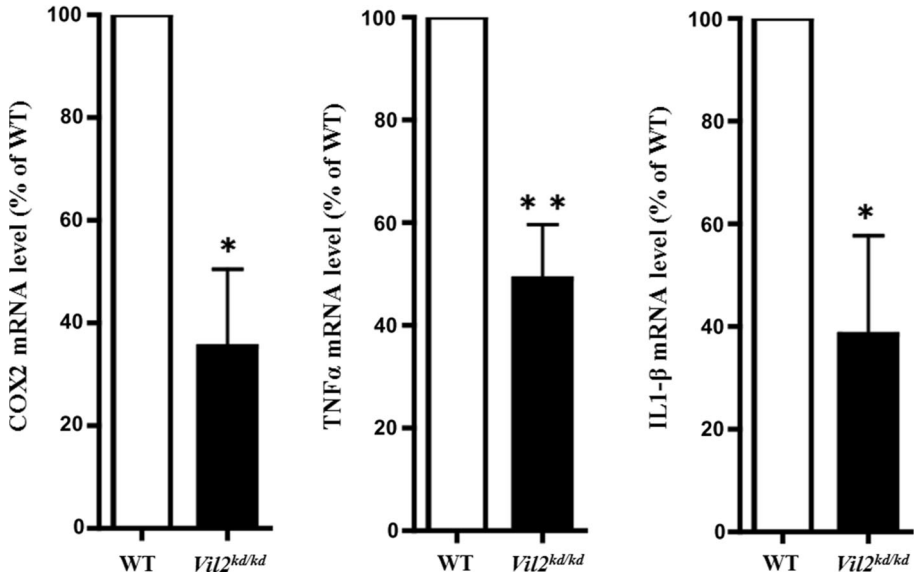

Fig. 6 mRNA expression levels of COX-2, TNF-α, and IL-1β in the gastric corpus were compared between wild-type and *Vil2*$^{kd/kd}$ mice. The mRNA expression levels were normalized to the expression level of GAPDH, and values are shown as percentages of the expression levels in the wild-type. All values are mean ± SE, $N = 3$, for wild-type and *Vil2*$^{kd/kd}$ mice. $^{*}P < 0.05$ and $^{**}P < 0.01$ versus wild-type

the decrease in the number of parietal cells was not large in the *Vil2*$^{kd/kd}$ mice. In addition, *Vil2*$^{kd/kd}$ parietal cells lacked typical tubulovesicles, and subsets of these cells contained abnormal vacuoles and abnormal round-shaped mitochondria (Fig. 7). Abnormal ultrastructure of parietal cells after targeted disruption of genes for gastric proton

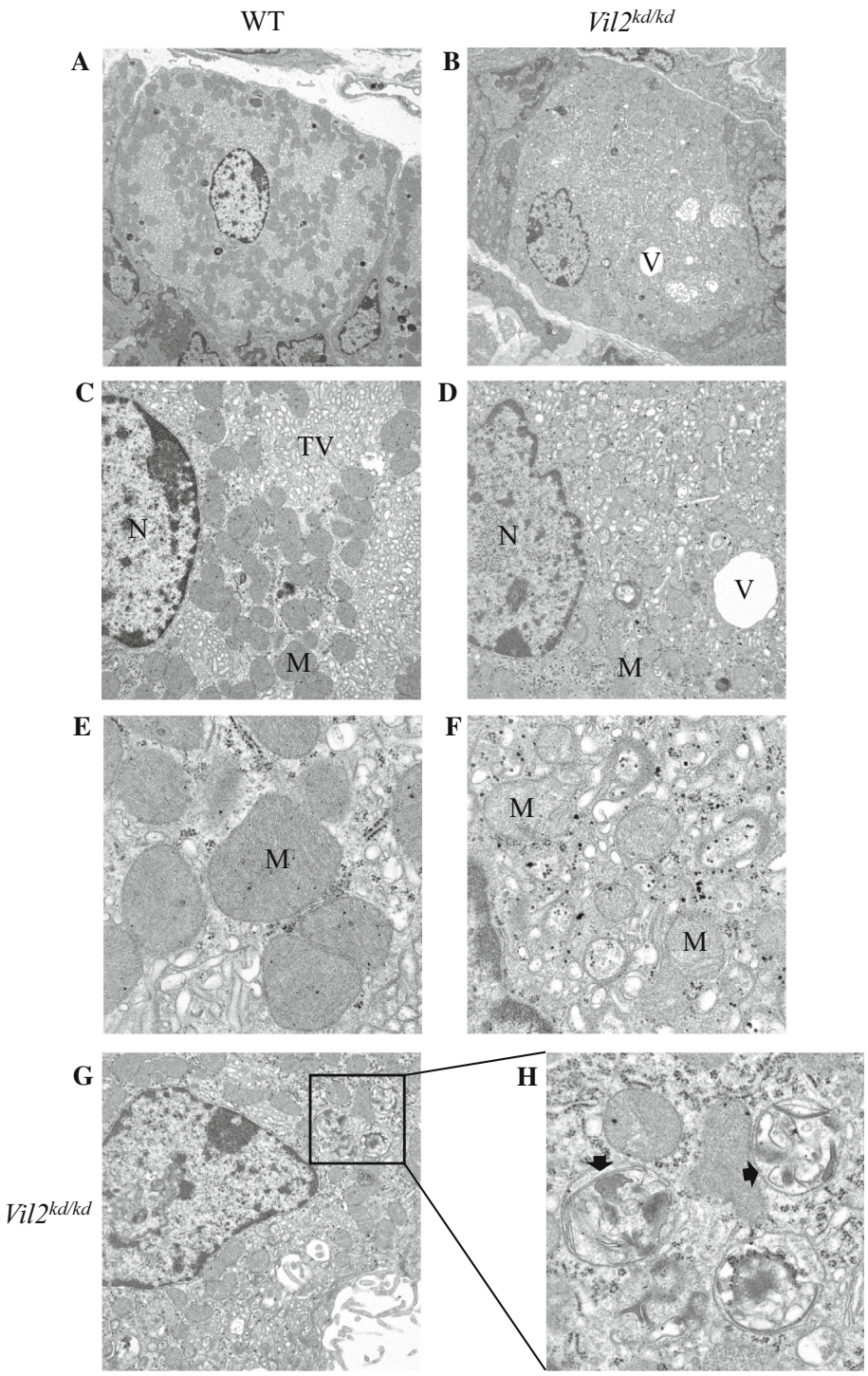

Fig. 7 Ultrastructure of parietal cells of wild-type (**a**, **c**, **e**) and *Vil2*$^{kd/kd}$ (**b**, **d**, **f**) mice at different magnifications. **a**, **b** Low magnifications (×3610) of parietal cells. **c**–**f** Higher magnifications of parietal cells (**c**, **d** ×9300; **e**, **f** ×31,800). **g**, **h** Abnormal multilamellar structures (*arrows*) were observed in the parietal cells of *Vil2*$^{kd/kd}$ mice at low (×9300) (**g**) and high (×31,800) (**h**) magnification. *N* nucleus, *M* mitochondrion, *TV* tubulovesicle, *V* vacuolar structure

pump α and β subunits and KCNE2 has been reported elsewhere [19–21].

It should be noted that abnormal multilamellar structures, which were similar to autophagosomes, were found in the subsets of parietal cells (Fig. 7g, h). Autophagy is up-regulated when cells need to generate intracellular nutrients under starvation and rid themselves of damaging cytoplasmic compartments [38]. Autophagy of ER membranes has, in fact, been induced by agents that promote ER stress [39]. Selective degradation of peroxisomes by autophagy has also been observed in hepatocytes isolated from clofibrate-treated rats [40]. In our study, autophagy may be up-regulated to remove abnormal vesicular structures or mitochondria in the parietal cells of *Vil2*$^{kd/kd}$ mice. Further study is necessary to precisely identify these structures in *Vil2*$^{kd/kd}$ mouse parietal cells.

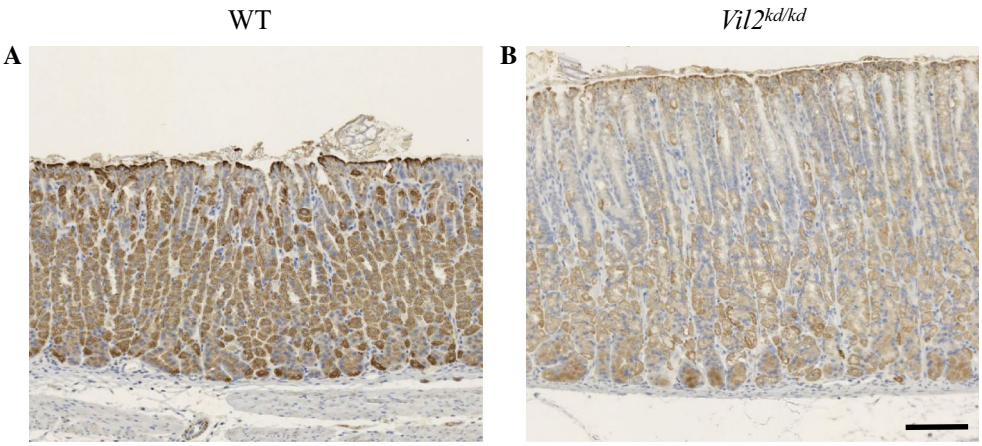

Fig. 8 Expression of mitochondrial complex IV subunit I in the gastric corpus of wild-type (**a**) and *Vil2*$^{kd/kd}$ (**b**) mice. Sections of the gastric corpus of wild-type and *Vil2*$^{kd/kd}$ mice were stained with the anti-OxPhos Complex IV subunit I (1D6E1A8) antibody. *Scale bar* 100 μm

In conclusion, foveolar hyperplasia, dilation of the fundic gland, decrease in the percentage of chief and parietal cells, and an increase in the percentage of neck cells were observed in the *Vil2*$^{kd/kd}$ mouse stomach. These changes may be a secondary effect of achlorhydria. In the parietal cell of *Vil2*$^{kd/kd}$ mice, severe perturbations in the secretory membranes were observed. Therefore, ezrin expressed in parietal cells is involved not only in the normal structure of the secretory membranes of the parietal cell but also in the normal structure of gastric epithelia.

Acknowledgments We thank Professor Tsukita for giving us the *Vil2*$^{kd/kd}$ mice. We thank Dr Yosuke Matsumoto, Mr Hiroki Murakami, Ms Karin Ikeda, and Ms Kaori Akiyama for their help with breeding and genotyping of mice and for technical support. This research was supported in part by Grants-in-Aid for Scientific Research (21590082 and 24590104) from the Ministry of Education, Culture, Sports, Science and Technology of Japan to S.A., and a High-Tech Research Center Project for Private Universities: matching fund subsidy from the Ministry of Education, Culture, Sports, Science and Technology of Japan to S.A.

Compliance with ethical standards

Conflict of interest The authors declare that there is no conflict of interest.

Ethical approval All work with animals was performed with the approval of the Animal Ethics Committees of Ritsumeikan University.

References

1. Bretscher A, Edwards K, Fehon RG (2002) ERM proteins and merlin: integrators at the cell cortex. Nat Rev Mol Cell Biol 3:586–599
2. Fehon RG, McClatchey AI, Bretscher A (2010) Organizing the cell cortex: the role of ERM proteins. Nat Rev Mol Cell Biol 11(4):276–287
3. Tsukita S, Yonemura S (1999) Cortical actin organization: lessons from ERM (ezrin/radixin/moesin) proteins. J Biol Chem 274:34507–34510
4. Sato N, Funayama N, Nagafuchi A, Yonemura S, Tsukita S, Tsukita S (1992) A gene family consisting of ezrin, radixin and moesin. Its specific localization at actin filament/plasma membrane association sites. J Cell Sci 103:131–143
5. Andréoli C, Martin M, Le Borgne R, Reggio H, Mangeat P (1994) Ezrin has properties to self-associate at the plasma membrane. J Cell Biol 107:2509–2521
6. Gary R, Bretscher A (1995) Ezrin self-association involves binding of an N-terminal domain to a normally masked C-terminal domain that includes the F-actin binding site. Mol Biol Cell 6:1061–1075
7. Berryman M, Franck Z, Bretascher A (1993) Ezrin is concentrated in the apical microvilli of a wide variety of epithelial cells whereas moesin is found primarily in endothelial cells. J Cell Sci 105:1025–1043
8. Hanzel DK, Urushidani T, Usinger WR, Smolka A, Forte JG (1989) Immunolocalization of an 80-kDa phosphoprotein to the apical membrane of gastric parietal cells. Am J Physiol (Gastrointest Liver Physiol) 256:G1082–G1089
9. Hanzel D, Reggio H, Bretscher A, Forte JG, Mangeat P (1991) The secretion-stimulated 80 K phosphoprotein of parietal cells is ezrin, and has properties of a membrane cytoskeletal linker in the induced apical microvilli. EMBO J 10(9):2363–2373
10. Zhou R, Cao X, Watson C, Miao Y, Guo Z, Forte JG, Yao X (2003) Characterization of protein kinase A-mediated phosphorylation of ezrin in gastric parietal cell activation. J Biol Chem 278(37):35651–35659
11. Saotome I, Curto M, McClatchey AI (2004) Ezrin is essential for epithelial organization and villus morphogenesis in the developing intestine. Dev Cell 6:855–864
12. Casaletto JB, Saotome I, Curto M, McClatchey AI (2011) Ezrin-mediated apical integrity is required for intestinal homeostasis. Proc Natl Acad Sci 108(29):11924–11929
13. Tamura A, Kikuchi S, Hata M, Katsuno T, Matsui T, Hayashi H, Suzuki Y, Noda T, Tsukita S, Tsukita S (2005) Achlorhydria by ezrin knockdown: defects in the formation/expansion of apical canaliculi in gastric parietal cells. J Cell Biol 169(1):21–28
14. Hatano R, Fujii E, Segawa H, Mukaisho K, Matsubara M, Miyamoto K, Hattori T, Sugihara H, Asano S (2013) Ezrin, a membrane cytoskeletal cross-linker, is essential for the regulation of phosphate and calcium homeostasis. Kidney Int 83:41–49
15. Hatano R, Akiyama K, Tamura A, Hosogi S, Marunaka Y, Caplan MJ, Ueno Y, Tsukita S, Asano S (2015) Knockdown of ezrin causes intrahepatic cholestasis by the dysregulation of bile fluidity in the bile duct epithelium. Hepatology 61(5):1660–1671
16. Dockray GJ, Varro A, Dimaline R, Wang T (2001) The gastrins: their production and biological activities. Annu Rev Physiol 63:119–139

17. Pagliocca A, Hegyi P, Venglovecz V, Rackstraw SA, Khan Z, Burdyga G, Wang TC, Dimaline R, Verro A, Dockray GJ (2008) Identification of ezrin as a target of gastrin in immature mouse gastric parietal cells. Exp Physiol 93:1174–1189
18. Schultheis PJ, Clarke LL, Meneton P, Harline M, Boivin GP, Sternmermann G, Duffy JJ, Doetschman T, Miller ML, Shull GE (1998) Targeted disruption of the murine Na^+/H^+ exchanger isoform 2 gene causes reduced viability of gastric parietal cells and loss of net acid secretion. J Clin Invest 101(6):1243–1253
19. Scarff KL, Judd LM, Toh B-H, Gleeson PA, van Driel IR (1999) Gastric H^+, K^+-adenosine triphosphatase β subunit is required for normal function, development, and membrane structure of mouse parietal cells. Gastroenterology 117:605–618
20. Spicer Z, Miller ML, Andringa A, Riddle TM, Duffy JJ, Doetschman T, Shull GE (2000) Stomachs of mice lacking the gastric H, K-ATPase α-subunit have achlorhydria, abnormal parietal cells, and ciliated metaplasia. J Biol Chem 275(28):21555–21565
21. Roepke TK, Anantharam A, Kirchhoff P, Busque SM, Young JB, Geibel JP, Lerner DJ, Abbott GW (2006) The KCNE2 potassium channel ancillary subunit is essential for gastric acid secretion. J Biol Chem 281(33):23740–23747
22. Judd LM, Andringa A, Rubio CA, Spicer Z, Shull GE, Miller ML (2005) Gastric achlorhydria in H/K-ATPase-deficient (*Atp4a*(−/−)) mice causes severe hyperplasia, mucocystic metaplasia and upregulation of growth factors. J Gastroenterol Hepatol 20:1266–1278
23. Karam SM, Straiton T, Hassan WM, Leblond CP (2003) Defining epithelial cell progenitors in the human oxyntic mucosa. Stem Cells 21:322–336
24. Falk P, Roth KA, Gordon JI (1994) Lectins are sensitive tools for defining the differentiation programs of mouse gut epithelial cell lineages. Am J Physiol Gastrointest Liver Physiol 266(29):G987–G1003
25. Zhu L, Hatakeyama J, Zhang B, Makdisi J, Ender C, Forte JG (2009) Novel insights of the gastric gland organization revealed by chief cell specific expression of moesin. Am J Physiol (Gastrointest Liver Physiol) 296:G185–G195
26. Gawenis LR, Ledoussal C, Judd LM, Prasad V, Alper SL, Stuart-Tilley A, Woo AL, Grisham C, Sanford LP, Doetschman T, Miller ML, Shull GE (2004) Mice with a targeted disruption of the AE2 Cl^-/HCO_3^- exchanger are achlorhydric. J Biol Chem 279(29):30531–30539
27. Goldenring JR, Nomura S (2006) Differentiation of the gastric mucosa III. Animal models of oxytic atrophy and metaplasia. Am J Physiol (Gastrointest Liver Physiol) 291:G999–G1004
28. Hattori T (1986) Development of adenocarcinomas in the stomach. Cancer 57:1528–1534
29. Longman RJ, Douthwaite J, Sylvester PA, Poulsom R, Corfield AP, Thomas MG, Wright NA (2000) Coordinated localization of mucins and trefoil peptides in the ulcer associated cell lineage and the gastrointestinal mucosa. Gut 47:792–800
30. Ding X, Deng H, Wang D, Zhou J, Huang Y, Zhao X, Yu X, Wang M, Wang F, Ward T, Aikhionbare F, Yao X (2010) Phospho-regulated ACAP4-ezrin interaction is essential for histamine-stimulated parietal cell secretion. J Biol Chem 285:18769–18780
31. Fujisawa S, Romin Y, Barlas A, Petrovic LM, Turkekul M, Fan N, Xu K, Garcia AR, Monette S, Klimstra DS, Erinjeri JP, Solomon SB, Manova-Todorova K, Sofocleous CT (2014) Evaluation of YO-PRO-1 as an early marker of apoptosis following radiofrequency ablation of colon cancer liver metastasis. Cytotechnology 66:259–273
32. Kakei N, Ichinose M, Tatematsu M, Shimizu M, Oka M, Yahagi N, Matsushima M, Kurokawa K, Yonezawa S, Furihata C, Shiokawa K, Kageyama T, Miki K, Fukamachi H (1995) Effects of long-term omeprazole treatment on adult rat gastric mucosa—enhancement of the epithelial cell proliferation and suppression of its differentiation. Biochem Biophys Res Commun 214:861–868
33. Nomura S, Yamaguchi H, Ogawa M, Wang TC, Lee JR, Goldenring JR (2005) Alterations in gastric mucosal lineages induced by acute oxyntic atrophy in wild-type and gastrin-deficient mice. Am J Physiol (Gastrointest Liver Physiol) 288:G362–G375
34. Jain RN, Al-Menhali AA, Keeley TM, Ren J, El-Zaatari M, Chen X, Merchant JL, Ross TS, Chew CS, Samuelson LC (2008) Hip1r is expressed in gastric parietal cells and is required for tubulovesicle formation and cell survival in mice. J Clin Invest 118:2459–2470
35. Wang TC, Goldenring JR, Dangler C, Ito S, Mueller A, Jeon WK, Koh TJ, Fox JG (1998) Mice lacking secretory phospholipase A2 show altered apoptosis and differentiation with *Helicobacter felis* infection. Gastroenterology 114:675–689
36. Lopez-Diaz L, Hinkle KL, Jain RN, Zavros Y, Brunkan CS, Keeley T, Eaton KA, Merchant JL, Chew CS, Samuelson LC (2006) Parietal cell hyperstimulation and autoimmune gastritis in cholera toxin transgenic mice. Am J Physiol (Gastrointest Liver Physiol) 290:G970–G979
37. Goldenring JR, Ray GS, Coffey RJ, Meunier PC, Haley PJ, Barnes TB (2000) Car BD (2000) Reversible drug-induced oxyntic atrophy in rats. Gastroenterology 118:1080–1093
38. Levine B, Kroemer G (2008) Autophagy in the pathogenesis of disease. Cell 132:27–42
39. Klionsky DJ (2007) Autophagy: form phenomenology to molecular understanding in less than a decade. Nat Rev Mol Cell Biol 8:931–937
40. Nardacci R, Sartori C, Stefanini S (2000) Selective autophagy of clofibrate-induced rat liver peroxisomes. Cytochemistry and immunocytochemistry on tissue specimens and on fractions obtained by nycodenz density gradient centrifugation. Cell Mol Biol 46:1277–1290